JOURNAL OF SOLID STATE CHEMISTRY 52, 124–129 (1984)

Synthesis and Solid State Studies on $Mb_2Sb_2O_7$ and $(Mn_{1-x}Cd_x)_2Sb_2O_7$ Pyrochlores

M. A. SUBRAMANIAN AND A. CLEARFIELD

Department of Chemistry, Texas A&M University, College Station, Texas 77843

A. M. UMARJI AND G. K. SHENOY

Materials Science and Technology Division, Argonne National Laboratory, Argonne, Illinois 60439

AND G. V. SUBBA RAO

Materials Science Research Center, Indian Institute of Technology, Madras 600 036, India

Received August 24, 1983; in revised form November 21, 1983

Pyrochlore oxides of the type $Mn_2Sb_2O_7$ and $(Mn_{1-x}Cd_x)_2Sb_2O_7$ have been synthesized by high-temperature solid state reactions and characterized by X-ray diffraction and chemical analysis. X-Ray diffraction studies showed that the compound $Mn_2Sb_2O_7$ has a rhombohedrally distorted pyrochlore structure. In the solid solutions $(Mn_{1-x}Cd_x)_2Sb_2O_7$, the phases with $x \geq 0.6$ are cubic. Magnetic and ^{121}Sb Mössbauer studies indicate that all the Mn and Sb are present in the +2 and +5 state occupying *A* and *B* sites, respectively, in the pyrochlore structure. Electrical measurements indicate that the compounds are insulators or semiconductors exhibiting *p*-type behavior. The stoichiometry and probable cause of the rhombohedral distortion in $Mn_2Sb_2O_7$ and solid solutions are discussed.

Introduction

Pyrochlore oxides of the type $A_2^{2+}B_2^{5+}O_7$, where *A* = Cd, Hg, Ca, Pb, or Sn and *B* = V, Nb, Ru, Rh, Ta, Re, Os, Ir, U, or Sb, have been widely reported in the literature (*1*). The antimonates $Ca_2Sb_2O_7$ and $Cd_2Sb_2O_7$ crystallize with structures of both the pyrochlore and weberite type (*2, 3*), whereas the $Hg_2Sb_2O_7$ is only known as a pyrochlore (*4*). Pb^{2+}-containing pyrochlore antimonates have been examined by many workers and found to be nonstoichiometric due to the presence of Pb^{4+} and Sb^{3+} (*5*). Brisse *et al.* (*6*) described the formation of $Mn_2Sb_2O_7$, having a cubic pyrochlore structure, by Baccaredda's method of preparation, viz. reacting Mn-acetate and antimonic acid at low temperatures (<600°C). They reported that the pyrochlore phase was stable only to about 600°C and its powder pattern was not well defined. Aia *et al.* (*7*) examined the formation of fluoroantimonates of Ca, Cd, and Mn with pyrochlore structure. However, their X-ray study showed that the manganese fluoroantimonate (with 35% F substituted for O) contained reflections due to the presence of

0022-4596/84 $3.00

Mn_2O_3 and $MnSb_2O_6$ as impurities. The exact stoichiometry of this preparation was not known. In this paper, we report on the synthesis and formation of $Mn_2Sb_2O_7$ and a solid solution of the type $(Mn_{1-x}Cd_x)_2Sb_2O_7$ with pyrochlore structure. Some data on the electrical and magnetic properties are also included. ^{121}Sb Mössbauer spectra were also recorded on some of the samples to ascertain the valence states of Sb in these pyrochlores.

Experimental

Synthesis. High purity starting materials used were $MnCO_3$ 99.999% (Puratronic grade J&M), Sb_2O_3 99.999% (Aldrich), CdO 99.99% (Ventron Corp). The starting materials in the stoichiometric proportions were thoroughly ground in an agate mortar and heated in Pt crucibles at 600°C for 6 hr to decompose $MnCO_3$ and to 900°C to oxidize Sb_2O_3 to Sb_2O_5. The samples were again ground thoroughly and packed in Pt tubes (4 mm i.d.) and sealed to prevent the evaporation Sb or Cd at high temperatures. The Pt tubes were heated to 1100°C for 20 hr.

X-Ray diffraction and chemical analysis. X-Ray powder diffraction patterns were taken with a PAD-II (Scintag) computer-controlled automated diffractometer using Cu$K\alpha$ radiation (λ = 1.5418 Å). The patterns were run by step-scanning the samples at 0.03°/5 sec and the position of the each peak was determined by program PEAK SEARCH (locally modified) supplied with the PAD-II. In all cases, Si powder (NBS-SR 640, a = 5.43088 Å) was used as the internal standard. The lattice parameters were obtained by least-squares fitting of 20 accurately determined d-spacings, using program LSCURE (*8*). The Mn, Cd, and Sb contents were determined by inductively coupled plasma arc analysis (ICPA) after dissolving the samples in 4 M HNO_3.

Mössbauer, electrical, and magnetic measurements. The antimony (^{121}Sb) Mössbauer experiments were carried out at 4.2 K in transmission geometry using $^{121}SnO_2$ source. The 37.15-KeV resonance γ rays were detected by counting the 9-KeV escape peak in a Xe–CO_2 proportional counter. The Mössbauer spectra were measured using a conventional electromechanical drive coupled to an ND-6600 computer. To avoid absorber thickness effects (*9*), only 5 mg/cm^2 of natural Sb was taken and diluted with boron nitride. Electrical resistivity, ρ (by two probe method) and Seebeck coefficient, α (by static method) measurements were performed on samples in the form of sintered pellets with Pt paint coated on both sides of the samples. Details of the equipment and measurement techniques have been described elsewhere (*10*). Magnetic susceptibility (χ) measurements, in the range 77–300 K, were performed using a Faraday balance. Alternating current (ac) magnetic susceptibility measurements were performed down to 4.2 K to check for any magnetic transitions.

Results

Single-phase $Mn_2Sb_2O_7$ could be prepared easily under the conditions employed. It was greenish yellow in color and the X-ray diffraction pattern indicated the compound to have the pyrochlore structure. A face-centered rhombohedral cell with lattice parameters a = 10.133(1) Å and α = 90.5(1)° gave an excellent accounting of the line splitting observed in the X-ray diffraction patterns. The indexed powder pattern on the basis of a hexagonal cell is given in Table I. The pycnometrically measured density for $Mn_2Sb_2O_7$ (using nitrobenzene as immersion liquid) is in very good agreement with the calculated value from the lattice constants (d_{meas} = 5.89 g/cm^3, d_{cal} = 5.94 g/cm^3) and gave Z = 8 for the face-centered rhombohedral cell. Chemical analysis for Mn and Sb by the ICPA method agrees well with the expected values on the

TABLE I

X-RAY DIFFRACTION PATTERN FOR $Mn_2Sb_2O_7$ BASED ON HEXAGONAL INDEXING (a_H = 7.196 Å, c = 17.397 Å)

$h\ k\ l$	d_{obs} (Å)	d_{cal} (Å)	I/I_0
1 0 1	5.872	5.867	10
0 0 3	5.804	5.799	13
1 0 2	5.070	5.066	14
1 0 3	4.250	4.245	3
1 1 0	3.597	3.598	5
1 0 4	3.570	3.567	7
2 0 1	3.066	3.067	10
1 0 5	3.040	3.038	3
2 0 2	2.933	2.934	100
0 0 6	2.900	2.900	37
2 0 4	2.532	2.533	41
2 1 4	2.070	2.071	2
1 0 8	2.053	2.053	2
2 2 0	1.799	1.799	22
2 0 8	1.784	1.783	20
2 2 3	1.718	1.718	3
1 0 10	1.677	1.676	2
4 0 1	1.551	1.551	3
4 0 2	1.533	1.534	11
2 2 6	1.529	1.529	15
2 0 10	1.520	1.519	10
4 0 4	1.467	1.467	7
0 0 12	1.450	1.450	3
3 2 2	1.411	1.411	2
4 0 8	1.266	1.267	5
3 1 10	1.226	1.226	2
1 0 14	1.218	1.219	2

basis of the chemical formula, $Mn_2Sb_2O_7$ (observed Mn, 23.5; Sb, 52.5; calculated Mn, 23.6; Sb, 52.5%; ratio Mn/Sb = 1.01).

Attempts were also made to synthesize solid solutions of the type $(Mn_{1-x}Cd_x)_2Sb_2O_7$. The other end member $Cd_2Sb_2O_7$ has been studied by many workers (*2, 3, 11*) and known to adopt both the pyrochlore and weberite structures depending on the temperature at which the synthetic procedure is carried out. Under our experimental conditions (at 1100°C) we found only the formation of weberite (orthorhombic, a = 7.215(1), b = 7.841(1), c = 10.188(1) Å) as reported earlier. Desgardin *et al.* (2) reported that the $Cd_2Sb_2O_7$ is apparently nonstoichiometric with a formula $Cd_{1.90}Sb_2O_{6.90}$ with some Sb existing in the 3+ state. In $(Mn_{1-x}Cd_x)_2Sb_2O_7$, we found that the substitution of Cd in $Mn_2Sb_2O_7$ progressively changed the crystal symmetry from rhombohedral to cubic. The complete transition

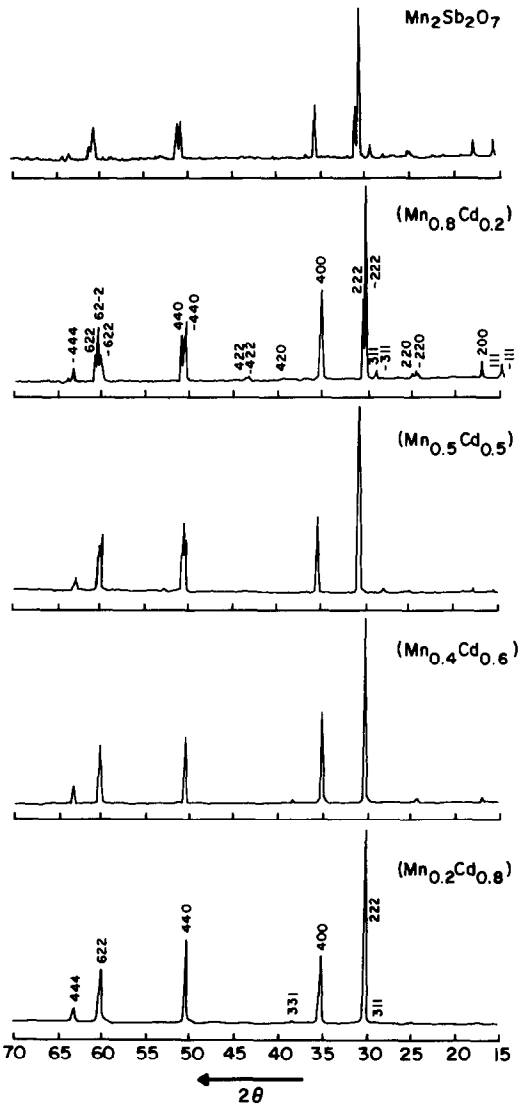

FIG. 1. X-Ray diffraction patterns of $Mn_2Sb_2O_7$ and $(Mn_{1-x}Cd_x)_2Sb_2O_7$ pyrochlores.

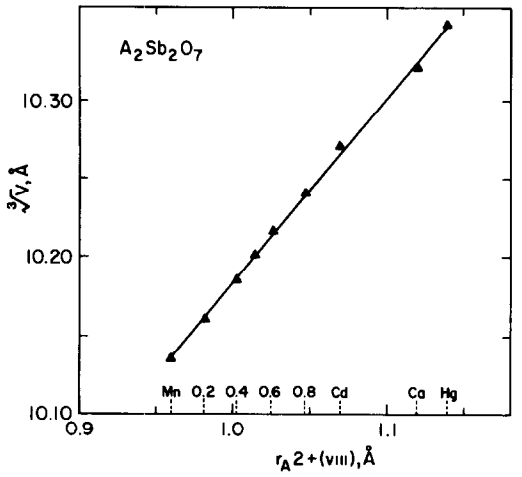

FIG. 2. Ionic radius vs unit cell size plot for $A_2Sb_2O_7$ pyrochlores.

occurs at $x \sim 0.6$. The X-ray diffraction patterns of the solid solutions are shown in Fig. 1. The nonconventional face-centered rhombohedral *hkl* values are indicated for comparison. A plot of unit cell parameters (as $\sqrt[3]{V}$ for the rhombohedral cell) vs r_A2+ (VIII) ionic radius (*12*) for $A_2Sb_2O_7$ pyrochlores gave a straight line with A = Hg, Ca, Cd falling on the same line (Fig. 2). The lattice parameters are listed in Table II. It is interesting to note that a small amount of Mn^{2+} substitution for Cd^{2+} in $Cd_2Sb_2O_7$ (even when $x = 0.1$) stabilizes the pyrochlore structure at 1100°C. Our attempts to synthesize $Cd_2Sb_2O_7$ with the pyrochlore structure at low temperatures (~800°C) gave X-ray diffraction patterns which were not well defined and the purity of the phase could not be established.

^{121}Sb Mössbauer spectra recorded on some representative samples in the $(Mn_{1-x}Cd_x)_2Sb_2O_7$ solid solution, i.e., x = 0.0, 0.2, and 0.8, showed only a single Mössbauer resonance line. A satisfactory computer fit to the data could be obtained by least-squares analysis using a single Lorentzian (Fig. 3). The observed isomer shifts with respect to $^{121}SnO_2$ and experimental linewidths are given in Table III.

Two probe electrical resistivity data obtained on dense sintered pellets in the range 300–700 K indicated that the compounds are insulators or semiconductors with $\rho_{300\ K} \sim 10^6$–10^8 ohm cm and the activation energy (E_a) obtained from Arrhenius plots (log ρ vs $1/T$) ranging from 0.5 to 0.7 eV. Although the absolute values of resistivity obtained on powder compacted specimens are not very reliable due to the complications arising from porosity and grain boundary effects, the trends in the ρ–T and E_a data shown by a related series of compounds prepared and measured in pellet form could be taken as real and significant. We find that in $(Mn_{1-x}Cd_x)_2Sb_2O_7$ ρ and E_a

TABLE II

UNIT CELL PARAMETERS AND ELECTRICAL PROPERTIES OF $(Mn_{1-x}Cd_x)_2Sb_2O_7$ PYROCHLORES

x in $(Mn_{1-x}Cd_x)_2Sb_2O_7$	a, Å (± 0.001)	$\alpha°$ (± 0.03)	$\rho_{300\ K}$ (ohm cm)	E_a (eV)
0.0	10.133	90.50	2.2×10^6	0.47
0.2	10.159	90.39	8.3×10^6	0.51
0.4	10.182	90.24	2.9×10^7	0.53
0.5	10.201	90.14	2.5×10^7	0.53
0.6	10.214	90	1.6×10^8	0.60
0.8	10.240	90	5.0×10^8	0.60
0.9	10.255	90	4.0×10^8	0.65
1.0[a]	10.273	90	—	—

[a] Values taken from Ref. (*3*).

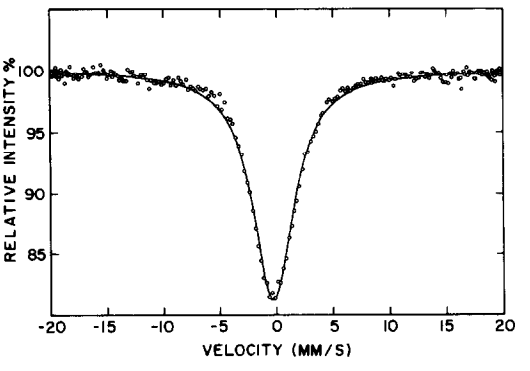

FIG. 3. ^{121}Sb Mössbauer spectra for $Mn_2Sb_2O_7$ at 4.2 K.

TABLE III

^{121}Sb MÖSSBAUER DATA FOR $(Mn_{1-x}Cd_x)_2Sb_2O_7$ PYROCHLORES

Compound	Isomer shift[a] (mm/sec)	Width (mm)
$Mn_2Sb_2O_7$	0.27(0.01)	4.30(0.1)
$(Mn_{0.8}Cd_{0.2})_2Sb_2O_7$	0.26(0.02)	4.11(0.1)
$(Mn_{0.2}Cd_{0.8})_2Sb_2O_7$	0.45(0.02)	4.63(0.12)

[a] Isomer shifts are with respect to $^{121}SnO_2$ source. Values in parentheses are errors.

increase as x is increased from 0.0 to 0.9. The electrical data are also given in Table II. Seebeck coefficient measurements indicated p-type conductions in all the samples and because of their high resistivity, reliable α values could not be obtained.

Magnetic susceptibility measurements on $Mn_2Sb_2O_7$ in the range 77–300 K indicated a paramagnetic behavior throughout the temperature range obeying the Curie–Weiss law. The experimentally derived Curie constant, C, was 4.11 for Mn^{2+} and the observed magnetic moment (μ = 5.76 BM) is very close to spin only value for a high spin d^5 system. The paramagnetic Curie temperature obtained by extrapolating the $1/\chi$ vs T plot gave a value of −33 K. Alternating current magnetic susceptibility measurements down to 4.2 K did not show any magnetic transition in $Mn_2Sb_2O_7$.

Discussion

The general pyrochlore formula can be written as $A_2B_2O_6O'$. The A atom coordination is that of a distorted cube (AO_6O_2') and the B atoms are in octahedral coordination. The A–O' distance is always shorter than A–O distance in all known pyrochlores. Neglecting the A–O interaction, the pyrochlore structure can be viewed as consisting of two interpenetrating networks of A_2O' and B_2O_6. Bond distances vary in the order B–O < A–O' < A–O (*4*). However, vacancies in A and O' sites are common in pyrochlores (*13*) as the B_2O_6 network forms the "backbone" of the structure. In $Mn_2Sb_2O_7$, both Mn and Sb can exist in variable oxidation states giving rise to nonstoichiometric phases (oxidation of Mn^{2+} to Mn^{3+}, reduction of Sb^{5+} to Sb^{3+}).

It is known that hyperfine interaction parameters of 37.15-KeV level in ^{121}Sb are quite sensitive to details of chemical bonding and electron distribution around antimony (*14*). Studies on halides (*15*) and oxides (*16*) containing Sb(III) and Sb(V) show characteristic isomer shifts (*IS*) of −11 to −16 and 0 to −4 mm, respectively, when measured with a $^{121}SnO_2$ source. Two separate valence states have been identified in α-Sb_2O_4 with the help of Mössbauer spectroscopy (*16*). If the local environment is not symmetrical it will produce a quadrupole pattern made of eight superposed Lorentzians showing an asymmetric resonance pattern.

In the pyrochlores the cation distribution among larger, eight-coordinated and distorted 16*d* sites (B_0 as origin) and the smaller, six-coordinated and more regular 16*c* sites has been worked out in Sn–Nb–O and Sn–Ta–O systems using ^{119}Sn Mössbauer resonance (*17, 18*). The Sn^{2+} occupying the A site (16*d*) is seen as a quadrupole split doublet with $IS \sim 4$ mm and the smaller Sn^{4+} is seen as a singlet with $IS \sim 0$ relative to $CaSnO_3$ source. Even an estimate of the relative ratio of the two valence states can be derived from the temperature-dependence measurement. All our Mössbauer spectra show only one type of Sb with an isomer shift of ~0 mm with respect to $^{121}SnO_2$ indicating Sb to be in +5 state. There is no presence of Sb^{3+} to the extent of 1 part in 10^3 in any samples. A single Lorentzian fit to the data (Fig. 3) indicates Sb to be in a symmetric environment. A linewidth of about 4 mm, though larger than the minimum observable width of 3.0 mm/sec for the present source, is not unusual

for an oxide with large Debye temperature measured at 4.2 K.

The magnetic and Mössbauer data taken together indicate that the compound $Mn_2Sb_2O_7$ should be nearly stoichiometric with all the Sb present as Sb^{5+} in octahedral coordination sites and all the Mn^{2+} occupying the *A* site. Absence of Mn^{3+} (which is a Jahn-Teller ion) in the *B* site and Sb^{3+} in the *A* site (which has a $5s^2$ lone pair) indicate the rhombohedral distortion in $Mn_2Sb_2O_7$ is probably caused by the displacement of Mn–O′ network (presumably due to the small size of Mn^{2+}). This type of distortion is similar to one observed in $Cd_2V_2O_7$ pyrochlore by Sleight (*19*). This view is supported by the fact that other $A_2Sb_2O_7$ where A = Ca, Cd, Hg are cubic and the progressive substitution of Cd in $Mn_2Sb_2O_7$ decreases the rhombohedral distortion and when $x \geq 0.6$ the solid solutions are cubic. Recent studies by Knop *et al.* (*3*) on the formation of $A_2Sb_2O_7$ pyrochlores, A = Cd, Sr, Ca indicated that the formation of pyrochlore compounds primarily depend on the effective size of A^{2+} and the covalency of the *A*–O bond. It has been observed that small size and high electronegativity values favor pyrochlore formation.

The high electrical resistivity of $Mn_2Sb_2O_7$ indicates that the d^5 electrons of Mn^{2+} are highly localized. This is because the Mn–O′ linkage is linear throughout the structure (and hence *s–p* bonding predominates) and the Mn–O interaction is very weak, as shown by the magnetic data. The activation energy is presumably related to the hopping of charge carriers from one Mn to another.

Our attempts to synthesize $Mn_2Nb_2O_7$ and $Mn_2Ta_2O_7$ with pyrochlore structure have failed, possibly due to the larger size of Nb and Ta compared to Sb.

Acknowledgments

The work done at Texas A&M university was supported by NSF Grant DMR 80-25184, for which grateful acknowledgment is made. The part of the work done at Argonne National Laboratory was supported by the U.S. Department of Energy.

References

1. M. A. SUBRAMANIAN, G. ARAVAMUDEN, AND G. V. SUBBA RAO, *Progr. Solid State Chem.* **15,** 55 (1983).
2. G. DESGARDIN, C. ROBERT, AND B. RAVEAU, *C. R. (Paris) C* **279,** 403 (1970); *Canad. J. Chem.* **56,** 1665 (1975).
3. O. KNOP, G. DEMAZEAU, AND P. HAGENMULLER, *Canad. J. Chem.* **58,** 2221 (1980).
4. A. W. SLEIGHT, *Inorg. Chem.* **7,** 1704 (1968).
5. G. BURCHARD AND W. RÜDORFF, *Z. Anorg. Allg. Chem.* **447,** 149 (1978).
6. F. BRISSE, D. J. STEWART, V. SEIDL, AND O. KNOP, *Canad. J. Chem.* **50,** 3648 (1972).
7. M. A. AIA, R. W. MOONY, AND C. H. H. HOFFMAN, *J. Electrochem. Soc.* **110,** 1048 (1963).
8. LSUCRE, Least Square Unit Cell Refinements, Univ. Freiburg i, Br., West Germany (1972).
9. G. K. SHENOY AND J. M. FRIEDT, *Nucl. Instrum. Methods* **116,** 573 (1976); *Phys. Rev. Lett.* **31,** 419 (1973).
10. M. A. SUBRAMANIAN AND G. V. SUBBA RAO, *J. Solid State Chem.* **31,** 329 (1980).
11. J. Y. MOISAN, J. PANNETIER, AND J. LUCAS, *C. R. (Paris) C* **279,** 565 (1976).
12. R. D. SHANNON, *Acta Crystallogr. Sect. A* **32,** 751 (1976).
13. A. W. SLEIGHT, F. ZUMSTEG, J. R. BARKLEY, AND J. E. GULLEY, *Mater. Res. Bull.* **13,** 1247 (1978).
14. G. M. BANCROFT AND R. H. PLATT, *Advan. Inorg. Chem. Radiochem.* **15,** 59 (1972).
15. J. M. FRIEDT, G. K. SHENOY, AND M. BURGARD, *J. Chem. Phys.* **59,** 4468 (1973).
16. G. G. LONG, J. G. STEVENS, AND L. H. BROWN, *Inorg. Nucl. Chem. Lett.* **5,** 799 (1969).
17. D. J. STEWART, O. KNOP, R. E. MEADS, AND W. G. PARKER, *Canad. J. Chem.* **51,** 1041 (1973).
18. T. BRICHAL AND A. W. SLEIGHT, *J. Solid State Chem.* **13,** 118 (1975).
19. A. W. SLEIGHT, *Mater. Res. Bull.* **9,** 1185 (1974).